

Structure of Liquid SiO₂: A Measurement by High-Energy X-Ray Diffraction

Q. Mei,¹ C. J. Benmore,^{1,2} and J. K. R. Weber^{3,*}

¹*Intense Pulsed Neutron Source Division, Argonne National Laboratory, Argonne, Illinois 60439, USA*

²*X-Ray Science Division, Argonne National Laboratory, Argonne, Illinois 60439, USA*

³*Containerless Research, Inc., Evanston, Illinois 60202, USA*

(Received 1 November 2006; published 2 February 2007)

The x-ray structure factor for liquid SiO₂ has been measured by laser heating of an aerodynamically levitated droplet. The main structural changes of the melt compared to the room temperature glass are associated with an increase in the size of the SiO₄ tetrahedra, indicating a small reduction in the average Si-O-Si bond torsion angle and an expansion of the network between 5 and 9 Å. Strong directional bonds with little high temperature broadening and a high degree of intermediate range order are found to persist in the liquid state.

DOI: [10.1103/PhysRevLett.98.057802](https://doi.org/10.1103/PhysRevLett.98.057802)

PACS numbers: 61.20.-p, 61.10.Nz

Silica glass formed by quenching a viscous melt has been the subject of much interest because of its geological and technological importance. It is also a prototypical network forming glass whose structure can be understood in terms of a continuous network of corner shared SiO₄ tetrahedra, with a relatively narrow range of bond angle distributions and a high degree of intermediate range order. Despite its importance there have been no structural studies on SiO₂ in the liquid state at magmatic temperatures, although both classical and *ab initio* molecular dynamics simulations have been performed [1–3].

Pure silica has a glass transition temperature T_g of 1177 °C (the mean temperature at which this highly viscous liquid solidifies), a relatively high melting point of 1713 °C, and a boiling point of 2950 °C [4]. Performing accurate diffraction measurements on high temperature liquids presents many technical difficulties. In recent years this has been overcome by using levitation techniques, for example, in the case of liquid Al₂O₃ [5]. However, unlike molten alumina, which can be aerodynamically levitated without any significant sample loss for several hours, molten silica evaporates very quickly above 1870 °C [6]. For example, a 3 mm diameter sphere of liquid SiO₂ lost approximately half its mass in 2 min during the experiments performed in this study. Using a combination of aerodynamic levitation, high-energy x-ray diffraction, and fast, large area x-ray detectors we have measured the structure factor for molten silica. The liquid and glass structure factors are found to be very similar, with an intense first sharp diffraction peak (FSDP) observed in the melt spectra. The average size of the SiO₄ tetrahedra are found to increase in the liquid compared to the room temperature glass, and this is accompanied by a slight increase of the peak positions between 5 and 9 Å in the liquid radial distribution function.

Ab initio molecular dynamics (MD) simulations suggest that the most important aspect between the melt and glassy states is a transformation in the Si-O-Si bond angle distribution [2]. An increased distribution of large Si-O-Si

angles, and a tail extending to much smaller angles in the liquid, is only observed when the ionic and covalent character of the Si-O chemical bond is considered explicitly and is not seen in classical molecular dynamics simulations. The change in $\angle(\text{Si-O-Si})$ distribution is accompanied by a high temperature broadening, which appears as a factor of 2 to 3 increase of the peak widths in the partial pair distribution functions [2]. Otherwise the *ab initio* simulations are in qualitative agreement with classical simulations [3], which have suggested the persistence of intermediate range order, signified by a first sharp diffraction peak, in the high temperature molten state.

The sample environment was controlled using aerodynamic levitation and a 240 W continuous-wave CO₂ laser beam heating system. Similar techniques have been applied in prior work [7], but in this experiment we have integrated the system on a high-energy x-ray diffraction beam line. The incident energy was calibrated with known gamma ray sources using a Ge point detector and found to be 115.12 keV. The advantages of high-energy diffraction for bulk liquid and glass studies include negligible attenuation and multiple scattering effects on millimeter-sized samples and the ability to access large momentum transfers [8]. The levitator was enclosed in a stainless steel chamber equipped with Kapton windows that transmit x rays with low attenuation or scattering at this energy. The instrument was integrated with beam line 11 ID-C at the Advanced Photon Source. The experiment was performed in transmission geometry and diffraction patterns were collected using a Mar345 image plate detector mounted orthogonal to and centered about the x-ray beam to avoid complex oblique incident effects in the phosphor layer [9]. The direct beam was blocked with short length of 3 mm diameter tungsten rod that was mounted in front of the image plate.

Spherical SiO₂ samples 3–3.5 mm in diameter were levitated in a flow of pure oxygen gas and melted with the laser beam from above. An x-ray beam of 1 mm × 1 mm in size intercepted only the top of the sample, above

the levitation nozzle. The image plate was exposed for 30 s to capture the scattered photons from a molten droplet. This was performed for 10 samples and the runs were averaged to improve the counting statistics. Background measurements taken with no sample present and the laser off were dominated by scattering from levitation gas. No Bragg peaks from the levitation nozzle were observed in any spectra. Corrections to the scattered x-ray intensity were applied using the software FIT2D [10] and the x-ray structure factor, $S_X(Q)$, was obtained up to $Q \sim 18 \text{ \AA}^{-1}$ using the program PDFGETX2 [11]. The measured liquid and hot glass x-ray structure factors are almost identical [see Fig. 1 and the supplementary material for the tabulated $S(Q)$ data [12]] suggesting that most of the structural changes occur upon heating the glass, and there is no abrupt transformation in the average bond angle distributions upon melting [13,14]. These $S(Q)$'s are remarkably similar to the room temperature glass diffraction pattern, despite a slight broadening of the features, mostly in the first and second peaks. The main difference between the liquid and hot glass spectra is the shape of the second peak in $S_X(Q)$; see the inset of Fig. 1. Also shown is the value of $S(Q=0)$ determined by the isothermal compressibility at T_g . From this figure it is clear that the FSDP is largely intact in the melt spectra and that there is no significant

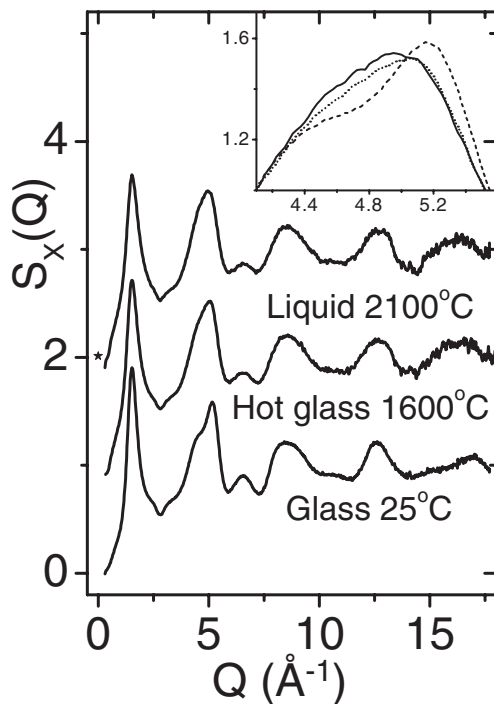


FIG. 1. Measured x-ray structure factors for liquid and glassy SiO_2 [13,14]. Inset: The main changes between the hot glass (dotted line) and liquid (solid line) occur in the shape of the second peak. The glass at room temperature (dashed line) is also shown. The star at $Q = 0 \text{ \AA}^{-1}$, $S(0) = 0.0123$ represents the value of the measured isothermal compressibility for the liquid at T_g [21].

change in its position, signifying the presence of a strong network in the liquid of the same periodicity to that observed in the glass, albeit slightly reduced in intensity.

The apparent temperature of the levitated sample was measured using an optical pyrometer that was carefully aligned to view the sample in the region where it was heated and coincident with the x-ray beam probe. The measured apparent temperature was corrected to obtain the true temperature using Wein's approximation to Planck's law. Temperature corrections were made for (i) reflections from surfaces of two pyrometer lenses, (ii) reflections from surfaces of a Pyrex window in the sample chamber, and (iii) the emissivity of the sample [15]. The calculated emissivity was 0.966 based on an index of refraction of 1.456. The average true temperature of the liquid was $2100 \text{ }^\circ\text{C}$, and the range of temperatures between different runs was $1960\text{--}2175 \text{ }^\circ\text{C}$. The estimated error due to emissivity and temperature gradients is $\pm 150 \text{ }^\circ\text{C}$. A potential source of error in temperature measurement was vaporization of the sample that produced smoke and condensate on the inside of the chamber window, which would result in an underestimate of temperature.

Figure 2 shows the x-ray radial distribution functions, $G_X(r)$, derived from the measured $S_X(Q)$ for liquid and glassy SiO_2 compared to those calculated from published data from classical and *ab initio* molecular dynamics simulations [2,3]. The inversion of $S_X(Q)$ to $G_X(r)$ was

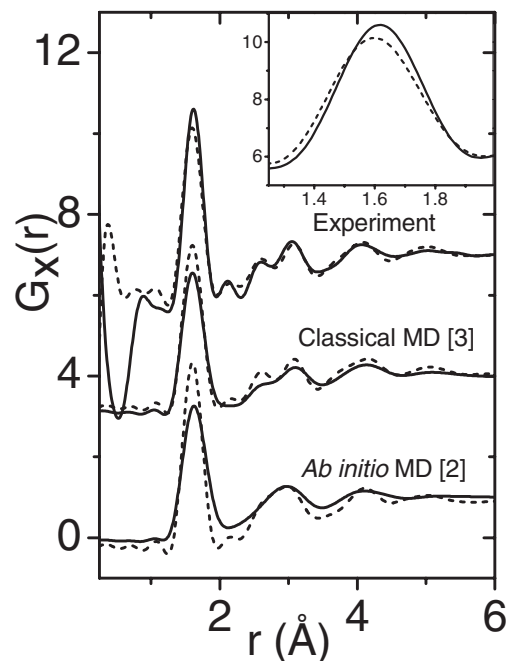


FIG. 2. X-ray radial distribution functions for liquid (solid lines) and glassy (dashed lines) SiO_2 . Top: Experiment. Middle: Classical molecular dynamics taken from Ref. [3]. Bottom: *Ab initio* molecular dynamics taken from Ref. [2]. Inset: Shift in experimental data of the Si-O peak.

performed in an identical manner for both the experimental and simulation data [16], using densities of 0.0620 \AA^{-3} for experimental data, 0.0631 \AA^{-3} for the *ab initio* simulation, and 0.0662 \AA^{-3} for classical MD simulation [2,3,19]. The first real peak in the x ray $G_X(r)$ is attributed to the Si-O bond, which elongates upon heating the glass from $1.597 \pm 0.005 \text{ \AA}$ at 25°C to $1.626 \pm 0.005 \text{ \AA}$ at 1600°C , and it remains at this value in the melt at 2100°C . This is in excellent agreement with *ab initio* molecular dynamics simulations, but is not predicted in classical simulations. Exarhos *et al.* [20] have observed a growth of a broad feature near 900 cm^{-1} in the Raman spectra consistent with an increased number of broken Si-O-Si linkages in the liquid; however, the average coordination numbers of the glass and liquid are found to be 3.90 ± 0.20 and 3.88 ± 0.20 , respectively, consistent with the predominance of SiO_4 tetrahedra. The Si-O bond breaking and reforming in the melt have been used to explain the viscous flow of high silicic aluminosilicate magmas, which is consistent with the jumplike diffusion process observed in *ab initio* molecular dynamics simulations of pure liquid SiO_2 [1,2].

The second peak in $G_X(r)$ is dominated by the O-O peak, which overlaps with the third peak due mainly to Si-Si correlations. It can be seen from the low- r side of the O-O peak that it shifts slightly to longer distances in the melt, and the high- r side of the Si-Si peak remains the same as in the glass. The decrease in the position of the third peak is therefore likely to be mainly associated with an increase of the O-O distance, and there is no clear evidence for a change in the Si-Si distance. A precise deconvolution of the O-O and Si-Si peaks from the x-ray data is problematic since the distributions are unlikely to be Gaussian [21]; however, it is clear that there is little change in the shape of these peaks between the liquid and glassy functions. It is more reliable to convert the partial pair distribution functions obtained in the simulations to reproduce the measured x-ray function, as shown in Fig. 2.

For the O-Si-O bond angle distribution, *ab initio* MD [2] has shown that in the range of the most probable bond angles the average bond length is approximately constant. This justifies taking the peak positions from the liquid x-ray radial distribution function to find the average $\angle(\text{O-Si-O})$, which is $107^\circ \pm 2^\circ$, showing that essentially tetrahedral symmetry is well maintained in the melt. However, both classical and *ab initio* simulations [2,3] show a large broadening of the Si-O, O-O, and Si-Si peaks between the glass and liquid, which leads to a much broader $\angle(\text{O-Si-O})$ and $\angle(\text{Si-O-Si})$ distributions. These peaks are much sharper in the experimental data and there is very little broadening between the glass and liquid $G_X(r)$ functions, indicating the persistence of strong directional bonds in the melt.

The first determination of the $\angle(\text{Si-O-Si})$ distribution in glassy SiO_2 was made by Mozzi and Warren [22] using x-ray diffraction data, assuming no correlation exists be-

tween bond length and bond angle. This approach has also been used by other groups as x-ray instrumentation has improved (e.g., see Neufeind *et al.* [23]). However, advances in NMR techniques by Clark and co-workers have recently suggested a strong positive correlation exists between the $\angle(\text{Si-O-Si})$ and Si-O bond length, in an opposite sense to that found in crystalline SiO_2 polymorphs [24–26]. These authors report an average $\angle(\text{Si-O-Si})$ of $\sim 147^\circ$ [24] in reasonable agreement with diffraction data [23]. As the temperature is increased, infrared absorption measurements on silica glass have shown that the position of the overtone at $\sim 2264 \text{ cm}^{-1}$ reaches a maximum around 950°C , suggesting that the average Si-O-Si bond angle reaches a maximum corresponding to a density minimum at this temperature [27]. At higher temperatures, above T_g , Raman spectroscopy measurements show the 440 cm^{-1} band increases in frequency, indicating a decrease in the average $\angle(\text{Si-O-Si})$ in the supercooled liquid regime [28]. From the shift in the Si-O peak in $G_X(r)$, assuming the Si-Si distance is invariant, a decrease in the average $\angle(\text{Si-O-Si})$ of $\sim 9^\circ$ is found in the melt compared to the room temperature glass, originating from the increased size of the tetrahedra alone.

The narrowness of the $\angle(\text{Si-O-Si})$ distribution has implications for ring topology. An average angle of $\sim 147^\circ$ in the glass is consistent with a topology dominated by 6-membered rings and few smaller rings. A significant broadening of the $\angle(\text{Si-O-Si})$ distribution to incorporate lower angles would be consistent with an increase in the population of 3-membered rings which range from 128° to 136° . Raman spectroscopy measurements by McMillan *et al.* [28] have shown that in the supercooled liquid the 606 cm^{-1} vibrational peak associated with 3-membered rings becomes more pronounced. Although these effects are in qualitative agreement with *ab initio* MD simulations, which show a skewed correlation towards small bond angles and short bond lengths in the melt compared to the glass, the limited change in the average torsion angles between SiO_4 tetrahedra inferred by the x-ray diffraction data and discussed above indicates that the melt is probably still dominated by 6-membered rings.

Correlations out to longer distances are shown in Fig. 3. Although the fine structure for $r > 6 \text{ \AA}$ is almost certainly spurious, there is a distinct overall shift in intensity to higher r for the peaks at approximate distances of 5.0, 6.3, 7.5, and 8.7 \AA in the function $rD_X(r)$ for liquid, where $D_X(r) = 4\pi\rho[G_X(r) - 1]$. This is consistent with an expansion of the network at lower densities, not clearly observed in the MD simulations. The strong FSDP in the structure factor for the melt and correlations to distances up to $\sim 10 \text{ \AA}$ indicate the persistence of significant intermediate range order, as predicted by classical simulations. We note that the primary local change in the x-ray radial distribution function for the SiO_2 glass at room temperature and the liquid at 2100°C is an increase in the size of

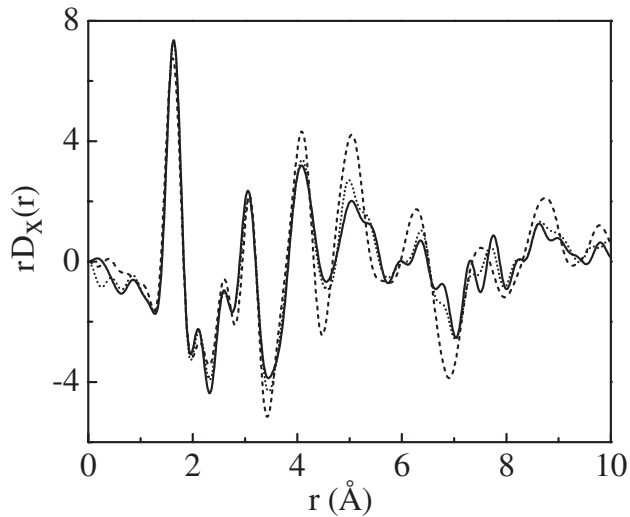


FIG. 3. The differential distribution function $D_X(r) = 4\pi\rho[G_X(r) - 1]$ multiplied by r [30] highlights the average deviations in structure from the bulk at longer distances. Correlations are observed out to 10 \AA in the melt. Room temperature glass (dashed line), hot glass (dotted line), and liquid (solid line).

the SiO_4 tetrahedra which is analogous to the effect in liquid water upon heating. The $\sim 1.7\%$ increase in the size of the tetrahedra observed in this study corresponds to a temperature shift of approximately 50°C in liquid water [29].

Dr. Joerg Neufeind of the Spallation Neutron Source is thanked for useful discussions. This work was supported by the U.S. DOE, at the XSD and IPNS Divisions, Argonne National Laboratory under Contract No. DE-AC02-06CH11357 and partially supported by NASA Contract No. NMM04AA23G.

*Present address: Materials Development, Inc., Arlington Heights, IL 60004, USA

- [1] J. Sarnthein, A. Pasquarello, and R. Car, Phys. Rev. Lett. **74**, 4682 (1995).
- [2] J. Sarnthein, A. Pasquarello, and R. Car, Phys. Rev. B **52**, 12 690 (1995).
- [3] P. Vashista, R. K. Kalia, and J. P. Rino, Phys. Rev. B **41**, 12 197 (1990).
- [4] *Handbook of Chemistry and Physics*, edited by D. R. Lide (CRC Press, Boca Raton, FL, 2006), 87th ed., pp. 4–88.
- [5] S. Ansell *et al.*, Phys. Rev. Lett. **78**, 464 (1997).
- [6] S. M. Schnurre, J. Grobner, and R. Schmid-Fretzer, J. Non-Cryst. Solids **336**, 1 (2004).
- [7] S. Krishnan *et al.*, Rev. Sci. Instrum. **68**, 3512 (1997).
- [8] H. F. Poulsen *et al.*, J. Non-Cryst. Solids **188**, 63 (1995).
- [9] J. Zaleski, G. Wu, and P. Coppens, J. Appl. Crystallogr. **31**, 302 (1998).
- [10] Computer code FIT2D, in A. P. Hammersley, European Synchrotron Radiation Facility, Grenoble, France, Internal Report No. ESRF98HA01T, 1998 (unpublished); see web site for details at <http://www.esrf.fr/computing/scientific/FIT2D/>
- [11] X. Qiu, J. W. Thompson, and S. J. L. Billinge, J. Appl. Crystallogr. **37**, 678 (2004).
- [12] See EPAPS Document No. E-PRLTAO-98-033707 for supplementary material for the tabulated $S(Q)$ data. For more information on EPAPS, see <http://www.aip.org/pubservs/epaps.html>.
- [13] The structure factor of the SiO_2 glass at room temperature was measured using an energy discriminating Ge point detector.
- [14] A change in background gas scatter was found between the high temperature sample runs and the empty instrument at room temperature, which manifested itself as a long wavelength slope on the spectra between $Q = 10$ and 20 \AA^{-1} . The $S(Q)$ data in Fig. 1 show the data with the unphysical low- r oscillations (below 1.20 \AA) removed. The real space distribution functions in Figs. 2 and 3 are direct Fourier transforms of the measured structure factors without this correction.
- [15] J. K. R. Weber *et al.*, J. Am. Ceram. Soc. **78**, 583 (1995).
- [16] The simulation partial pair distribution functions were digitized from Refs. [1,2], Fourier transformed into reciprocal space and multiplied by the corresponding Q -dependent Faber-Ziman weighting factors assuming the independent atom approximation [17]. The resulting x-ray diffraction total structure factor, $S_X(Q)$, was truncated at the same $Q_{\text{max}} = 17.6 \text{ \AA}^{-1}$, and Fourier transformed back into real space with a Lorch modification function [18].
- [17] H. Ohno *et al.*, J. Non-Cryst. Solids **293**, 125 (2001).
- [18] E. A. Lorch, J. Phys. C **2**, 229 (1969).
- [19] J. F. Bacon, A. A. Hasapis, and J. W. Wholley, Phys. Chem. Glasses **1**, 90 (1960).
- [20] G. Exarhos *et al.*, in *Proceedings of the 11th International Conference on Raman Spectroscopy*, edited by R. J. H. Clark and D. A. Long (John Wiley & Sons, Chichester, 1988), p. 503.
- [21] A. C. Wright, J. Non-Cryst. Solids **179**, 84 (1994).
- [22] R. L. Mozzi and B. E. Warren, J. Appl. Crystallogr. **2**, 164 (1969).
- [23] J. Neufeind and K.-D. Liss, Ber. Bunsenges. Phys. Chem. **100**, 1341 (1996).
- [24] T. M. Clark *et al.*, Phys. Rev. B **70**, 064202 (2004).
- [25] M. D. Newton and G. V. Gibbs, Phys. Chem. Miner. **6**, 221 (1980).
- [26] G. V. Gibbs, Am. Mineral. **67**, 421 (1982).
- [27] S. Sen *et al.*, Phys. Rev. Lett. **93**, 125902 (2004).
- [28] P. F. McMillan *et al.*, Geochim. Cosmochim. Acta **58**, 3653 (1994).
- [29] R. T. Hart *et al.*, Phys. Rev. Lett. **94**, 047801 (2005).
- [30] R. J. Dejus *et al.*, J. Non-Cryst. Solids **143**, 162 (1992).